NORCE Norwegian Research Centre AS
www.norceresearch.no

SCIENTIFIC ASSESSMENT OF TSCV RETRIEVAL FROM STEREO-SAR – RETRIEVAL ALGORITHM

Harald Johnsen

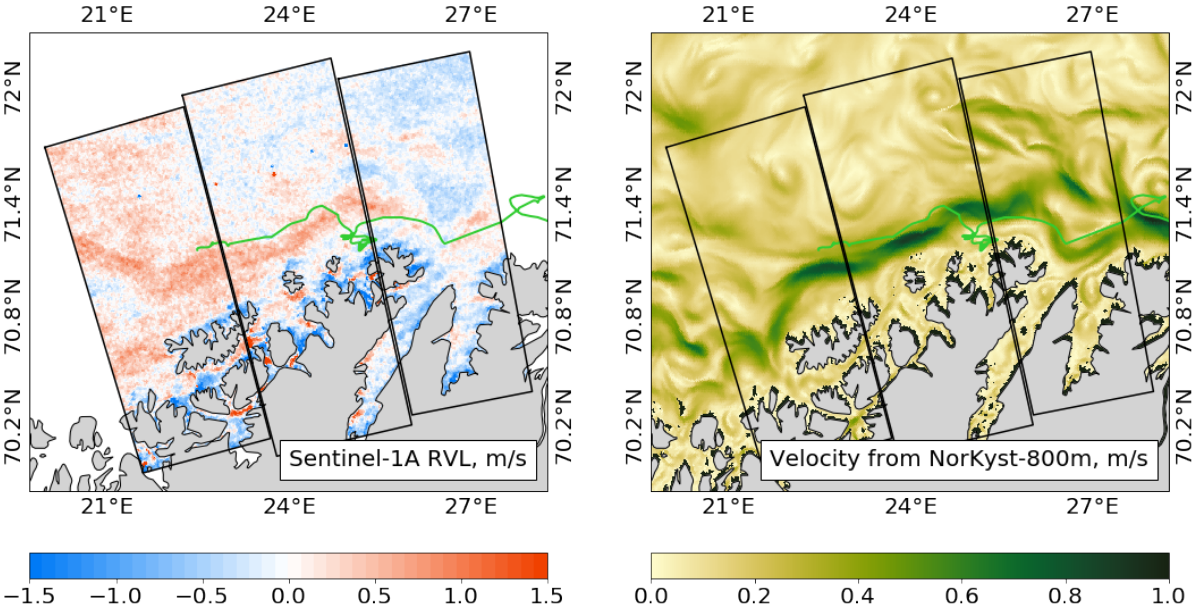

REPORT 1 – 2019

Project title:	Scientific Assessment of TSCV retrieval from stereo-SAR - retrieval algorithm
Project number:	101540
Institution:	NORCE Norwegian Research Institute, Tromsø
Client/s:	European Space Agency - ESTEC

Classification:	Open
Report no.:	1
ISBN:	978-82-8408-035-2
Number of pages:	19
Publication month:	October 2019

Resymé / Summary:

In this technical note we provide a detailed description of ocean current retrieval algorithm to be applied in the end-to-end performance simulator. The retrieval algorithm is based on the forward and retrieval models described in [R-5]. The technical note gives a detailed mathematical description and flowchart of the retrieval algorithm. This technical note refers to deliverable TN3, TN4 of the SATRoSS project.

Front page: Norwegian coastal current mapped with Sentinel-1A and modelled with Norkyst-800m. Surface drifter trajectory overlaid. Courtesy of A. Moiseev.

Revisions

Rev.	Date	Author	Checked by	Approved by	Reason for revision
1.0	3-Oct-19	H. Johnsen	K. A. Høgda		NA

Tromsø, 30.09.2019

Harald Johnsen	Kjell-Arild Høgda	Kjell-Arild Høgda
Project manager	*Quality assurance*	*Manager*

Contents

Abbreviations:

CS	-	Companion Satellite (cs1, cs2)
DC	-	Doppler Centroid
DCA	-	Doppler Centroid Anomaly
LBB	-	Long Baseline Bistatic
LBS	-	Long Baseline Stereostatic
NRCS	-	Normalized Radar Cross Section
NESZ	-	Noise Equivalent Sigma Zero
OSC	-	Ocean Surface Current
RAR	-	Real Aperture Radar
S1	-	Sentinel 1
SAR	-	Synthetic Aperture Radar
TSCV	-	Total Surface Current Vector
ISV	-	Integral cross spectral energy parameter
E2E	-	End-to-end

Reference Documents:

R-1 Scientific Assessment of TSCV Retrievals from Stereo-SAR (SATRoSS) - Statement of Work, ITT AO/1-8875/17/NL/AI, EOP-SM/3099, Issue 1, 27/02/2017

R-2 Fois F., "S1+CS Selected Concept Performance Analysis Report", S1CS.ASU.SY.PR.0000X, Issue 2.0, 2016

R-3 S1+CS Mission Requirements Document, S1CS.ASU.SY.RP.00001, Issue 2.0, August 2016

R-4 S1+CS Mission System Design and Analysis Report, S1CS.ASU.SY.RP.0006, Issue 2.1, January 2017

R-5 Scientific Assessment of TSCV Retrieval from Stereo-SAR : A critical review, Norut Report No. 4/2018, ISBN 978-82-7492-403-1, ISSN 1890-5226, 16.07.2018

R-6 Scientific Assessment of TSCV Retrieval from Stereo-SAR: Performance Definition, Technical Note, TU Delft, 2018

R-7 Elfouhaily T., B. Chapron, K. Katsaros, D. Vandemark (1997), A unified directional spectrum for long and short wind-driven waves, J. Geophys. Res.,Vol.102, No. C7, pp.15781-15796, 1997

R-8 Romeiser R., Thompson D. R., "Numerical study on the Along-Track Interferometric Radar Imaging Mechanism of Oceanic Surface Currents", IEEE Trans. Geo. Rem. Sensing, Vol.38, No.1, January 2000.

R-9 Hansen M.W., Kudryavtsev V., Chapron B., Johannessen J.A., Collard F., Dagestad K.F., Mouche A.A., Simulation of radar backscatter and Doppler shifts of wave–current interaction in the presence of strong tidal current. Remote Sensing of Environment, May 2012, Volume 120, Pages 113–122, http://dx.doi.org/10.1016/j.rse.2011.1

R-10 Moiseev A., Johnsen H., Hansen M. W. Hansen, Johannessen J.A., Evaluation of radial ocean surface currents derived from Sentinel-1 IW Doppler shift using coastal radar and Lagrangian surface drifter observations, Draft peer review paper, September 2019

R-11 Schulz-Stellenfleth J., "Ocean wave measurements using complex synthetic aperture radar data", PhD Thesis, University of Hamburg, 2003

R-12 Fouques S., Johnsen H., Krogstad H.E., "Influence of a nonlinear RAR modulation on the SAR imaging of ocean waves, Proc. of IGARSS'05, Seoul S. Korea, DOI:10.1109/IGARSS.2005.15252

R-13 Nilsen V., Engen G., Johnsen H. (2019), "A novel approach to SAR ocean wind retrieval", IEEE Transactions on Geoscience and Remote Sensing, ISSN: 1558-0644, Digital Object Identifier: 10.1109/TGRS.2019.2909838, 2019.

R-14 Li, H., Chapron, B., Mouche, A., & Stopa, J. E. (2019). A new ocean sar cross-spectral parameter: definition and directional property using the global sentinel-1 measurements. Journal of Geophysical Research: Oceans, in press. Retrieved from https://agupubs.onlinelibrary.wiley.com/doi/abs/10.1029/2018JC014638 doi: 10.1029/2018JC014638

R-15 Trové N., Koeniguer E. C., Fargette P., De Martino A., "Influence of geometrical configurations and polarization basis definitions on the analysis of bistatic polarimetric measurements", IEEE Transactions on Geoscience and Remote Sensing, Vol.49, No. 6, June 2011, doi: 10.1109/TGRS.2010.2093533

1. Introduction

One or two passive follower to the Sentinel 1 missions operating in ATI, LBB or LBS modes is a promising concept for measuring ocean surface wind and current vector from space. The basic observation concept is shown in Figure 1. In the technical note [R-5] we described the forward and retrieval models to be considered for the end-to-end performance simulator. Here we provide a detailed description of the retrieval algorithm.

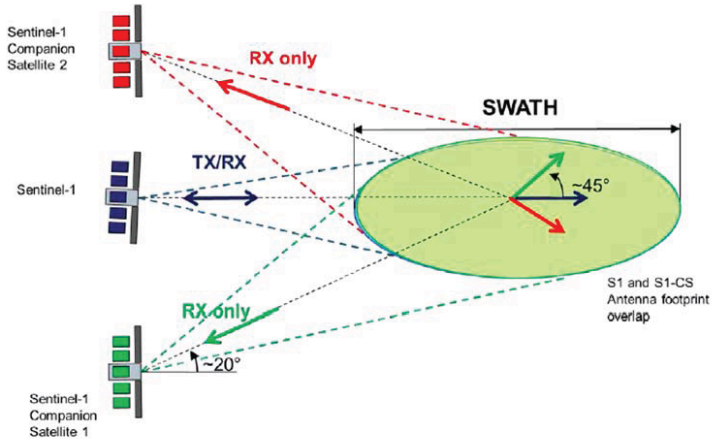

Figure 1 *Schematic illustration of the passive follower concept using a bistatic or stereostatic geometry with Sentinel-1. The figure is taken from [R-2]. When the transmit TX array is electronically steered in elevation or azimuth, the bistatic RX array is steered in 2D to achieve alignment of ground projected principal axis of TX and RX. Note that the effective azimuth bistatic scattering angle is roughly half the actual azimuth squint angles of the companions.*

2. Model Concept

In this study we have selected forward models based on the closed form approach. A description of the models can be found in [R-5]. This approach fits better to the main objectives of this study, which are the development of TSCV retrieval scheme and an end-to-end (E2E) performance simulator for the S1+CS observing system.

The GMFs to be used must be able to provide for both mono- and bistatic geometry and all linear polarizations (hh,vv,vh,hv), the following SAR metrics:

- Normalized radar cross section (NRCS)
- Doppler centroid anomaly (DCA) and Doppler spectra (or Doppler spread)
- Ocean wave image cross spectra (complex) (CCS)

The input parameters to the closed form GMFs selected for this study are *ocean wind vector*, *inverse wave age* and *surface current vector*. The ocean surface within the GMFs is described statistically with a wave spectra model (R-7). **Note that the forward NRCS, DCA and cross-spectra models used here do NOT include surface current implicitly i.e. current gradients and wave current interactions are not supported (R-8), (R-9) This is assumed to be a second order effect that can be neglected in an end-to-end performance simulator. However, for the DCA model the direct mean surface current contribution ($2\underline{\mathbf{k}}_{\mathbf{rad}} \cdot \underline{\mathbf{v}}$) is included as part of the retrieval model (see Eq.(2))**

Recent experiences with Sentinel IW data show that this retrieval methodology can provide high precision on the surface current (RMSe≈0.25 m/s) if wind vector estimate is achieved with sufficient precision (R-10).

The general parameterisation of the forward GMFs is:

$$(1) \quad GMF = \Gamma\left(U_{10}, \varphi.\underline{v}, \gamma, \theta_i, \theta_s, \phi_s, k_{rad}, pol\right)$$

where

- $U_{10} =$ wind speed $[m/s]$
- $\varphi =$ wind direction relative to range $[degRa]$
- $\underline{v} =$ surface current vector relative to range $[m/s]$
- $\gamma =$ inverse wave age $[norm]$
- $\theta_i =$ local radar beam incidence angle $(see\ Fig.2)[deg]$
- $\theta_s =$ local bistatic scattering elevation angle $(see\ Fig.2)[deg]$
- $\phi_s =$ local bistatic scattering azimuth angle $(see\ Fig.2)[deg]$
- $k_{rad} =$ radar wavenumber $[rad/m]$
- $pol =$ radar beam polarization $[hh, vv, hv, vh]$

The scattering geometry is illustrated in Figure 2. For the S1+CS LBS configuration the local bistatic scattering angle will always be in the range $90 < \phi_s < 270$. The S1+CS LBS observation geometry defining the incidence and azimuth angles is shown in Figure 3. The simulation is performed using exact S1 geometry (orbit). Some outputs of the forward model as function of along track baselines and wind speeds are shown in Figure 4 for NRCS and Figure 5 for DCA.

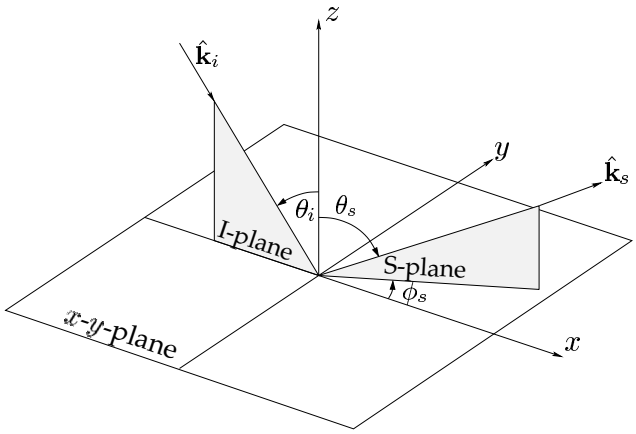

Figure 2 *General 3D bi-static scattering geometry. In the S1+CS system, the $\hat{k}_i$ defines the S1 radar wavenumber vector.*

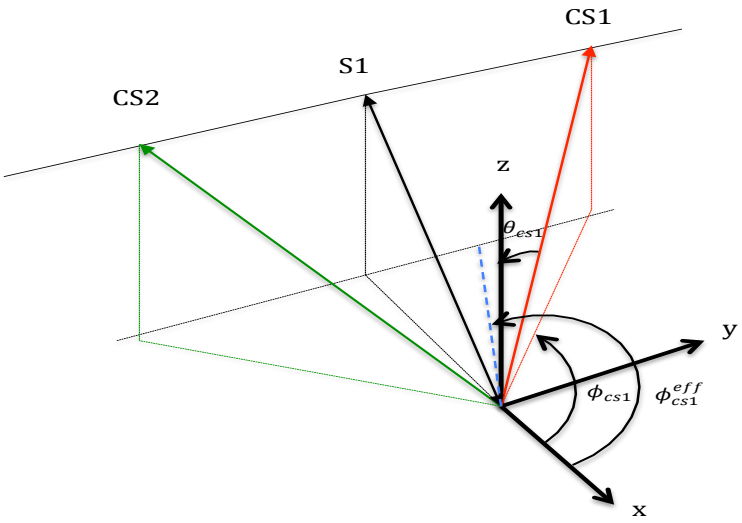

Figure 3 *S1+CS LBS observation geometry defining the incidence and azimuth angles. ϕ_{cs1}^{eff} is the effective bistatic scattering azimuth angle. Note that ϕ_{cs1}^{eff} is related to the physical azimuth squint angle ϕ_{cs1} i.e. 180-ϕ_{cs1}^{eff} ≈ (180-ϕ_{cs1})/2.*

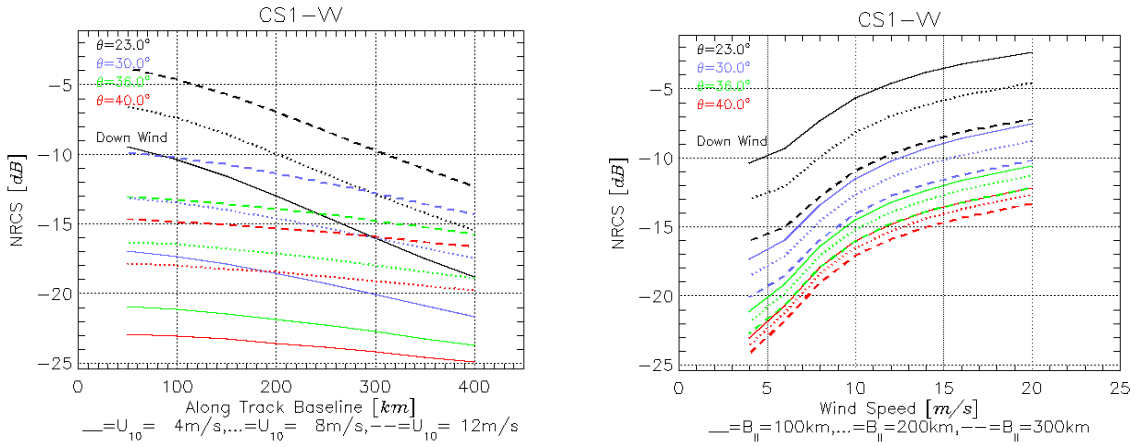

Figure 4 *Left: Predicted NRCS of companion as function of along track baseline for different incidence angles of S1 and wind speeds. Right: Predicted NRCS of companion as function of wind speed for different along track baseline and different incidence angles of S1. Wind direction is down wind.*

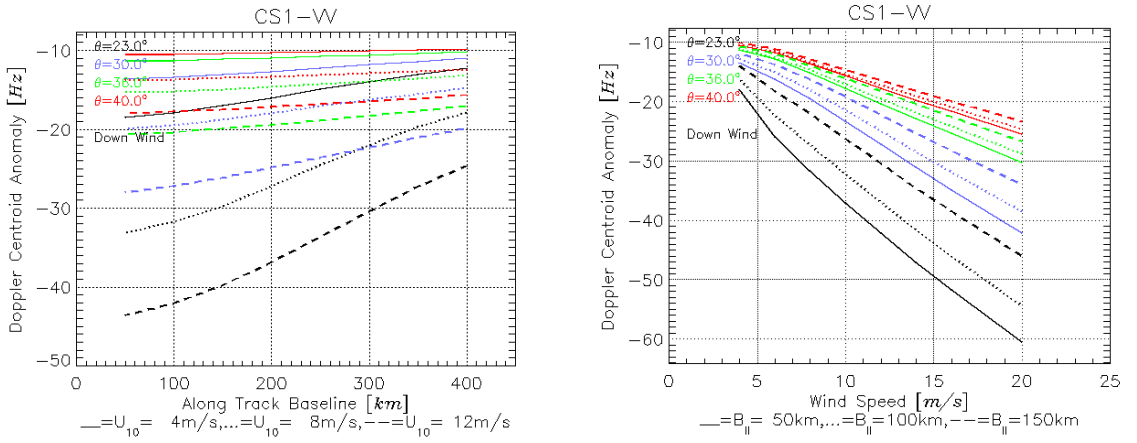

Figure 5 *Left: Predicted wind/wave DCA of companion as function of along track baseline for different incidence angles of S1 and wind speeds. Right: Predicted NRCS of companion as function of wind speed for different along track baseline and different incidence angles of S1. Wind direction is down wind.*

2.1. Model Parameter Relation

The uniqueness of the proposed S1+CS surface current retrieval is the use of the ocean wave image cross-spectral parameter (ISV) in combination with either the NRCS triplets or with both NRCS and DCA triplets. The ISV parameter is extracted from the imaginary part of the image cross spectra, $P(k_x, k_y; t)$ at range axis for wavelengths less than 30 meters (R-5), (R-13). The ISV parameter is a proxy for the signed range wind speed. By combining the ISV parameters with the triplets of NRCS from S1+CS, the wind vector can be retrieved without use of any ancillary information. The relation between these parameters and wind field as manifested in Sentinel-1 data is shown Figure 6, and simulated in Figure 7. We note some discrepancy between the simulated and measured parameters, in particular for the behavior of ISV parameter as function of wind speed. The forward spectral model predicts a linear behavior along range axis, while the observed data clearly indicates non-linear effects. A non-linear RAR model (R-11), (R-12) is currently under implementation in the forward

spectral model. The results will be evaluated against Sentinel-1 WV observations. Another option is to use an empirical forward model (mono-static) for the spectral parameter (R-13), (R-14). Since this empirical ISV model is based on an NRCS model, we can also foreseen to generate a similar ISV model for the companions using the bistatic simulated NRCS. A study on this approach is undertaken.

The Wind Scatterometer retrieval is also based on solving the NRCS triplets with respect to wind vector. However, ancillary wind direction from model (or in-situ) is required to remove the inherent 180^{o} ambiguity in the Scatterometer wind vector. The main benefit and the uniqueness of using the ISV parameter in combination with NRCS triplets, is its ability to resolve the line-of-sight wind direction ambiguity (i.e. signed range wind speed). The best option is to include in the minimization the triplets of ISV parameter, since for near range winds the azimuth ambiguity in the mono-static ISV parameter may not separate well (in case of noise) the ambiguity of the NRCS triplets. Secondly, for near azimuth winds the NRCS triplets do not separate well the wind direction, and triplets of ISV is needed to resolve the wind direction properly.

Any upgrade of the forward spectral model will not change anything in the retrieval scheme itself. The available forward bistatic scattering models have been released and published https://www.grss-ieee.org/publication-category/rscl/. A version of the Python code with increased throughput, S1 orbit geometry and an output (ncdf) module is available from the Gitlab repository at Norce.

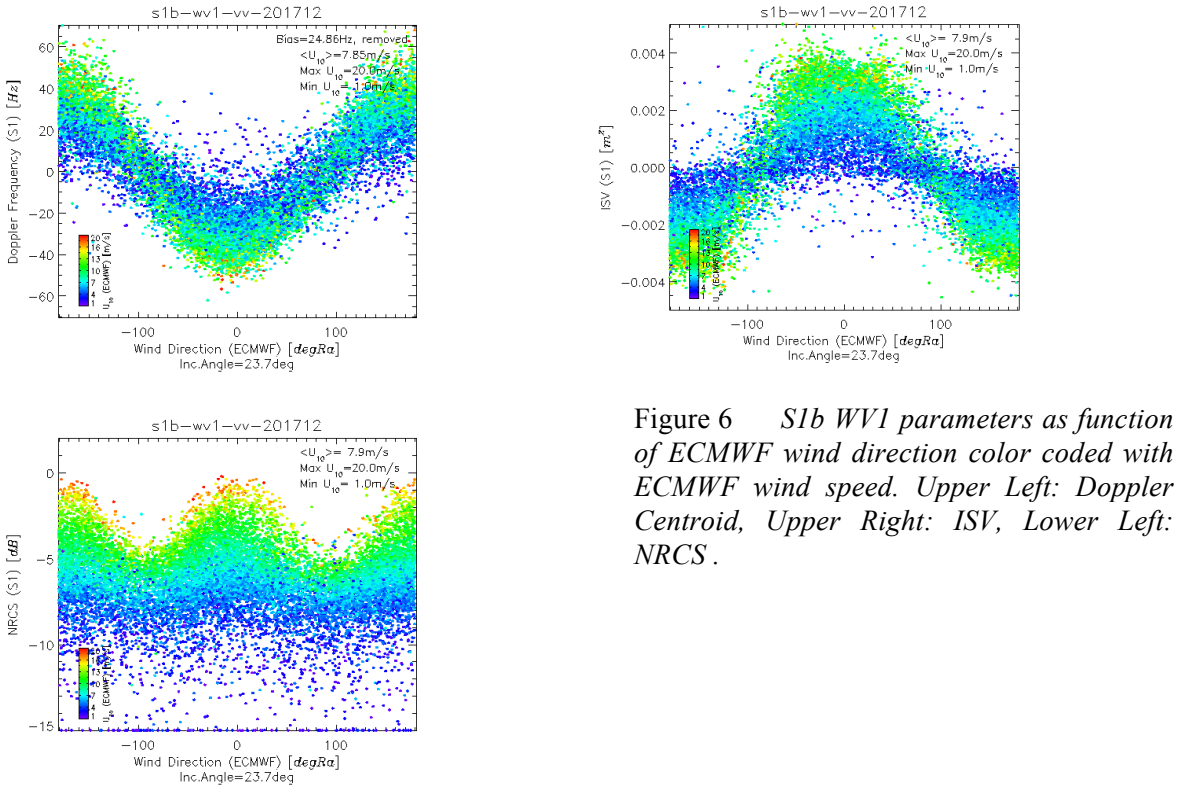

Figure 6 *S1b WV1 parameters as function of ECMWF wind direction color coded with ECMWF wind speed. Upper Left: Doppler Centroid, Upper Right: ISV, Lower Left: NRCS .*

The same parameters simulated using the closed form forward models are shown in Figure 7.

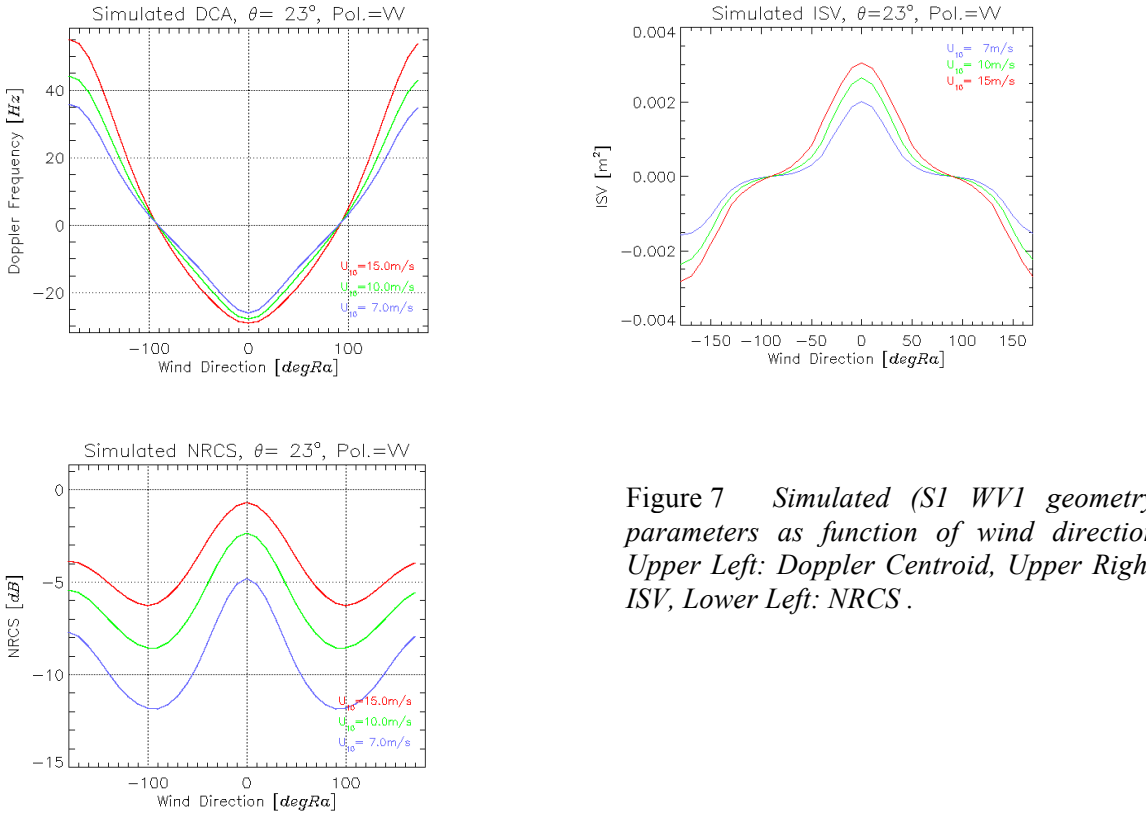

Figure 7 *Simulated (S1 WV1 geometry) parameters as function of wind direction. Upper Left: Doppler Centroid, Upper Right: ISV, Lower Left: NRCS .*

3. Retrieval Algorithm

The retrieval algorithm is based on the retrieval model outlined in the technical note [R-5], but simplified based on recent experiences with Sentinel-1 data. We have at this stage neglected the retrieval of wave age (i.e. we assume fully developed sea, $\gamma = \gamma_o = 0.84$) as well as skipping the use of the phase of the cross spectra for consistency check. This will be considered in the next version of the inversion scheme, when we better now how to model, extract and interpret "wave age" and "cross spectra phase" from the SAR measurements.

The concept of the TSCV retrieval algorithm is the combination of triplets of *NRCS, DCA* and the wind sea cross-spectral energy (*ISV*) from the S1+CS constellation. This approach avoids use of any external model wind field. Basically, use of the *ISV* parameter in the S1+CS constellation allows us solve for the 180° ambiguity in wind direction. The cost-function approach is similar to the one developed for the multi-antenna "WaveMill" (+/- 45 degree) system.

The revised retrieval scheme consist of the following steps:

Step 1. First iteration on wind vector

The first step is to provide a first iteration on $10m$ wind vector $\underline{U}_{10}$ from *NRCS* (σ) and image cross spectra energy (*ISV*) by minimization the cost function $J1$:

$$(1) \quad J1(\underline{U}_{10};\gamma_o) = \sum_{j\in\{s1,cs1,cs2\}} \frac{\left(\sigma^{(j)}_{o-mod}(\underline{U}_{10},\gamma_o)-\sigma^{(j)}_{o-obs}\right)^2}{Var\left(\sigma^{(j)}_{o-obs}\right)} + \frac{\left(isv^{(j)}_{mod}(\underline{U}_{10},\gamma_o)-isv^{(j)}_{obs}\right)^2}{Var\left(isv^{(j)}_{obs}\right)}$$

where the summation *j* is over the S1+CS measurements, and the subscript *mod* means the predicted GMF values and *obs* means the corresponding value estimated from the S1+CS data. Note that for the companions, the parameters need to be constructed as a combination of co- and cross-pol terms, even if the S-1 operates in single polarization mode. This is due to rotation of the polarization basis when going bistatic (R-15). Ideally, if the forward model can provide complex scattering coefficients, use of the covariance matrix could be foreseen for the bistatic measurements. However, for ocean surface the main contribution to the bistatic cross-pol signal comes from the geometry (rotation of polarization basis) and very little from the geophysical scattering process.

The spectral energy parameters, isv will be extracted from the wind driven sea region of the cross-spectra by integrating the imaginary part of the cross-spectra along range axis for wavelengths below 30m. The *Var* means the variance, which in general depends on the S1+CS system and measurements errors. The *Var* values will weight the various terms of the cost-function relative to each other. The wind direction is here relative to the range axis of S1 (transmitter). The *mod* data are pre-computed and stored in netCDF file. In Figure 8 we show example of the different terms of the cost-function in Eq.(1). We see how the combination of triplets of NRCS and one ISV parameter solves for the wind vector.

Step 2. First iteration on surface current radial components

The second step provides a first iteration of the surface current vector, $\underline{v}$. We start with estimating the expected *DCA wave bias* ($f_{dc-wave}$) using the forward *DCA* model with inputs $\underline{U}_{10}$ and $\gamma = \gamma_o$. Then we take the difference between observed *DCA* and the *DCA wave bias* and compute the first iteration on the radial surface current components for each of the three satellites:

$$(2) \quad v_r^{(j)} = -\frac{\pi\left(f_{dc-obs}^{(j)} - f_{dc-wave}^{(j)}\big|_{\underline{U}_{10},\gamma_o}\right)}{k_{rad}} \qquad j \in \{s1, cs1, cs2\}$$

where k_{rad} is radar wavenumber [rad/m].

We can now by using Eq.(6) construct the first estimate of surface current speed and direction.

Step 3. Refinement of wind vector

The third step performs a refinement of wind vector using the first iteration on surface current. First we perform a correction of measured *DCA* by subtracting the predicted *DCA* contribution caused by a steady surface current, $\underline{v}$:

$$(3) \quad \Delta f_{dc-obs}{}^{(j)} = f_{dc-obs}{}^{(j)} - \frac{1}{\pi}\left|\underline{k}_{rad}\right| v_r^{(j)} \qquad j \in \{s1, cs1, cs2\}$$

Then a cost-function minimization is performed for updating the $\underline{U}_{10}$:

$$(4) \quad J2\left(\underline{U}_{10}\right) = \sum_{j\in\{s1,cs1,cs2\}} \frac{\left(f_{dc-wave}^{(j)}(\underline{U}_{10},\gamma_o)\big|_{\underline{v}=0} - \Delta f_{dc-obs}^{(j)}\right)^2}{Var\left(\Delta f_{dc-obs}^{(j)}\right)} + \frac{\left(\sigma_{o-mod}^{(j)}(\underline{U}_{10},\gamma_o)\big|_{\underline{v}=0} - \sigma_{o-obs}^{(j)}\right)^2}{Var\left(\sigma_{o-obs}^{(j)}\right)} + \frac{\left(isv_{mod}^{(j)}(\underline{U}_{10},\gamma_o)\big|_{\underline{v}=0} - isv_{obs}^{(j)}\right)^2}{Var\left(isv_{obs}^{(j)}\right)}$$

The first term on RHS is the difference between the predicted "DCA Wave Bias" and the measured DCA compensated for the first guess current, $\underline{v}$. The second term is the difference between observed *NRCS* and modeled *NRCS* as function of $\underline{U}_{10}, \gamma = \gamma_o$. The third term is the difference between observed and modeled cross-spectral energy parameter as function of $\underline{U}_{10}, \gamma = \gamma_o$.

Step 4. Refinement of surface current radial components

The next step is a refinement of the estimated surface current components using the refined wind vector ($\underline{U}_{10}$) as inputs to the *DCA wave bias* model:

$$(5) \quad v_r^{(j)} = -\frac{\pi\left(f_{dc-obs}^{(j)} - f_{dc-wave}^{(j)}\big|_{\underline{U}_{10},\gamma_o,\underline{v}=0}\right)}{k_{rad}} \qquad j \in \{s1, cs1, cs2\}$$

These are the three surface radial current components that are used in the next step to construct the final estimate of the total surface current vector (TSCV).

Step 5. Total surface current vector

The final surface current vector, $\underline{v}$ in the azimuth, ground range plane $\left(\hat{\underline{x}}, \hat{\underline{y}}\right)$ (see Figure 10) is then established by combining the radial components, $v_r^{(j)}$ from mono-static and bistatic geometries as follows:

$$(6) \quad \phi = tan^{-1}\left(\frac{v_r^{cs2}/sin\theta_{cs2} - v_r^{cs1}/sin\theta_{cs1}}{2\, v_r^{s1} sin\,\psi_{cs}/sin\theta_{s1}}\right)$$

$$|\underline{v}| = \frac{v_r^{s1}}{sin\theta_{s1} cos\phi}$$

where ϕ is the surface current direction relative to S1 radar line of sight and $\psi_{cs} = \psi_{cs1} = -\psi_{cs2}$ is the effective bistatic angles between the S1 plane of incidence and the bisector planes of CS1 and CS2. And $\theta_{s1}, \theta_{cs1}, \theta_{cs2}$ are the incidence angles of S1 (i.e. in the plane of incidence) and of the CS1 and CS2 (i.e. in the bisector planes), respectively (see Figure 3). The relation between S1+CS radial surface current components and the total surface current vector is illustrated in Figure 10.

The current direction can furthermore be related relative to north as: $\phi = (\phi + \phi_{sat} + 90)\ MOD\ 360$ where ϕ_{sat} is the satellite heading relative to North.

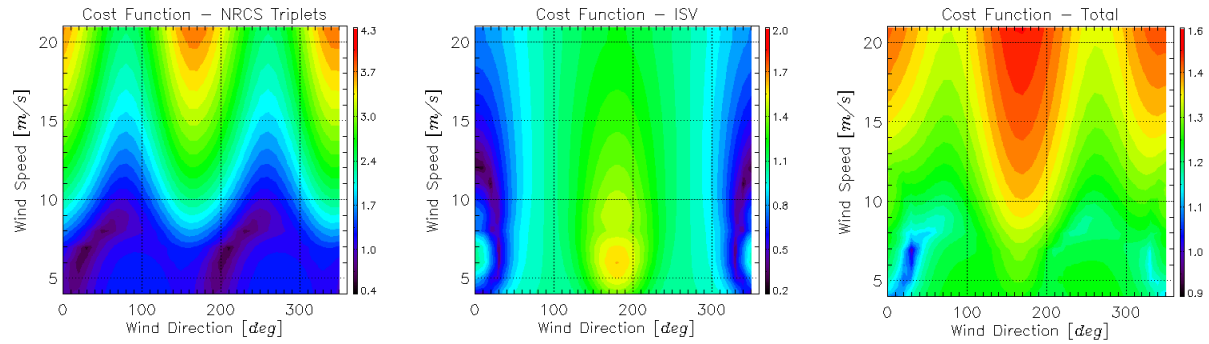

a) **b)** **c)**

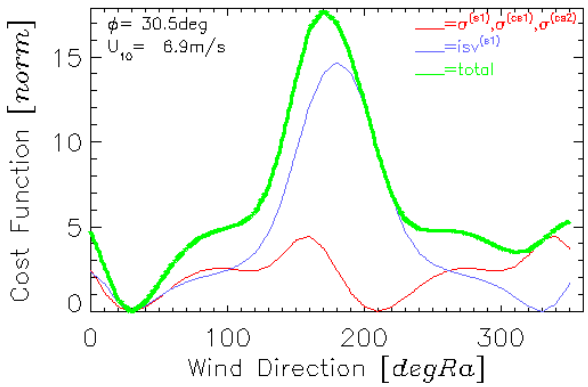

d)

Figure 8 *: Upper: The different cost-function terms (NRCS triplets (a), single ISV (b)) and the total cost-function (c) of Eq.(4) for a given wind speed of 7 m/s and wind direction of 30 degree relative to S1 range. Lower (d): Cost-function terms and total cost-function as function of wind direction for the wind speed that minimizes the total cost-function.*

We see from Figure 8a that the NRCS triplet cost-function contains a 180^o ambiguity in wind direction $(\phi, \phi + 180^o)$, while the single ISV (Figure 8b) contains an azimuth ambiguity in wind direction $(\phi, -\phi)$,. However, combining them solves out all the ambiguities and provide correct estimate of the wind vector (Figure 8c,d). One exception is when the wind direction is in azimuth since then the mono-static ISV parameter is zero. This is shown in Figure 9, where we show the cost functions for azimuth wind. We observe that for wind directions around azimuth (90, 270 degRa) the estimation of wind direction from minimization of cost-function is sensitive to noise. This is also manifested in the scatterplot of wind vector shown in Section 3.2.

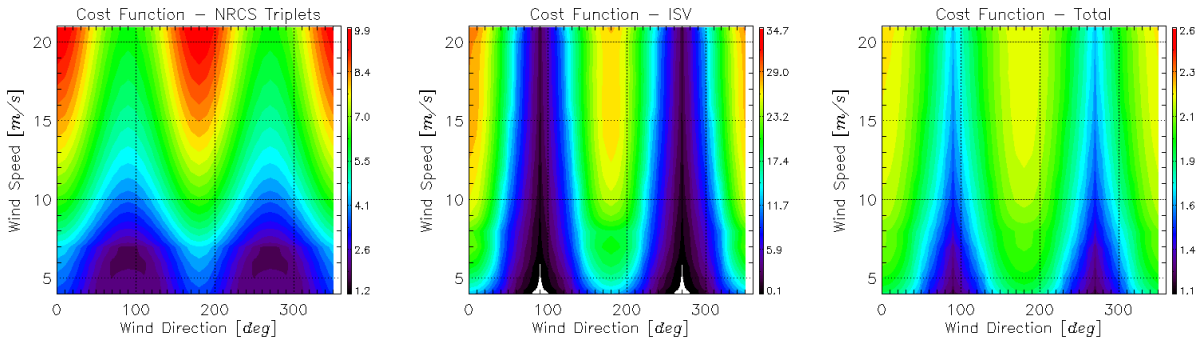

a) **b)** **c)**

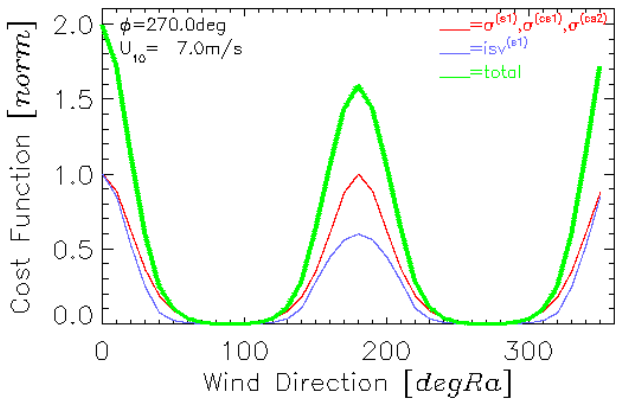

d)

Figure 9 *: Upper: The different cost-function terms (NRCS triplets (a), single ISV (b)) and the total cost-function (c) of Eq.(4) for a given wind speed of 7 m/s and wind direction of 90 degree relative to S1 range. Lower (d): Cost-function terms and total cost-function as function of wind direction for the wind speed that minimizes the total cost-function.*

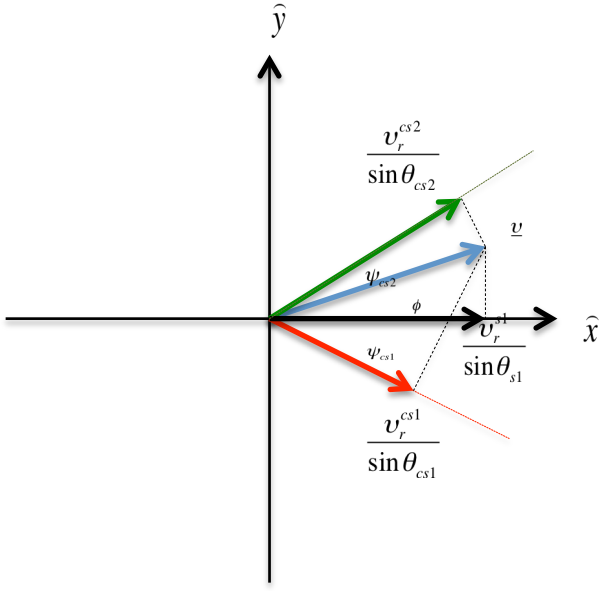

Figure 10 *Relation between the radial surface current vector components of S1+CS and the total surface current vector, $\underline{v}$ at an angle of ϕ with respect to S1 ground range. The bistatic azimuth scattering angles, ψ_{cs1}, ψ_{cs2} are the effective bistatic azimuth scattering angles. This is approximately half the azimuth squint angle of the companions relative to Sentinel-1.*

3.1. Implementation model

The implementation model of the retrieval scheme is described below. We have chosen to interface the forward and retrieval model via netCDF files. For each polarization, along track baseline and S1 swaths, separate netCDF files are generated for the S1, CS1 and CS2. We have here only considered the LBS configuration and VV & HH polarizations. A flowchart of the inversion model is shown in Figure 14.

3.1.1. Input Data

Forward Model Data:

The forward models are used to simulate NRCS, DCA and ISV parameters for different imaging geometries (S1+CS), polarizations and wind field conditions. Note that for the DCA, only the "DCA Wave Bias" is simulated. Contribution to DCA from a steady current is directly computed as part of the retrieval. The simulated data are stored in a netCDF file. The retrieval algorithm will read up the NRCS, DCA and ISV values for all wind conditions given the imaging geometry and polarization corresponding to the observed data of S1+CS system.

Observation Uncertainty:

With the total observation uncertainty (or precision) (Total Least Square) we mean the expected random geophysical error between the forward model and the corresponding observed NRCS, DCA and ISV parameters. These uncertainties should ideally also be dependent on the spatial resolution considered. The uncertainties are used to weight the different terms of the cost-function relative to each other. They are also used in the Monte Carlo simulation for generating random Gaussian noise. The total observation uncertainty is a combination of errors in the wind field (used as input to the forward model) and the natural variations of the air/sea conditions around the mean (in which the forward model is based on). The first contribution can be evaluated by simulating the sensitivity of the model outputs for small variations in the wind field. The latter can to some degree be assessed by estimating the variability of the observed (here we use S1 WV data) NRCS, DCA and ISV for given wind field. However, S1 WV data driven estimate will also include some variations due to errors in the collocated ECMWF wind field.

In the next figures we show S1 WV RMS variations of the NRCS (Figure 11), DCA (Figure 12) and ISV (Figure 13) as function of wind speed and direction for a bin size of 1 m/s and 15 degree, respectively. These RMS variations are adapted to the bistatic geometry by scaling with the corresponding ratio of mono- and bi-static mean values. We have generated these observation uncertainties for both VV and HH polarization using around 1 month of S1b WV acquisitions for each polarizations. We should note that most of the variations in the DCA are coming from attitude/pointing uncertainties. We use here instead the uncertainty of DCA of ≈ 2Hz achieved after careful calibration of the S1 WV DC using gyro data.

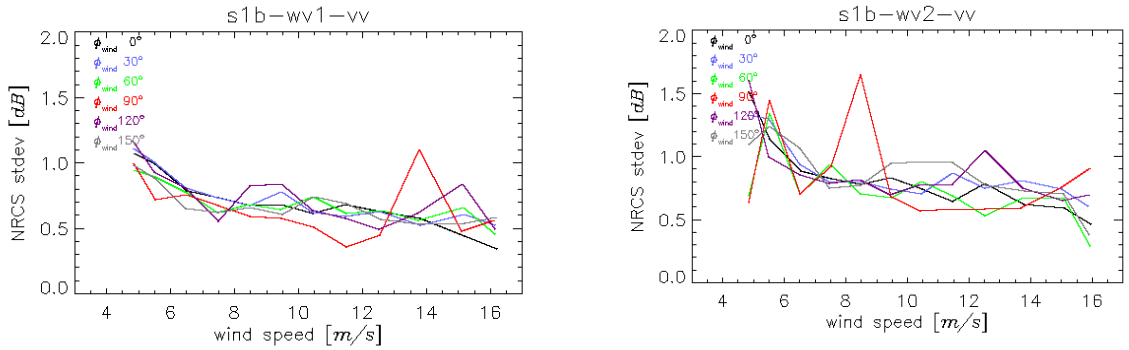

Figure 11 *S1 WV NRCS RMS variations as function of wind speed and wind direction. The variations are estimated over a bin of 1m/s in wind speed and 15 degree in wind direction.*

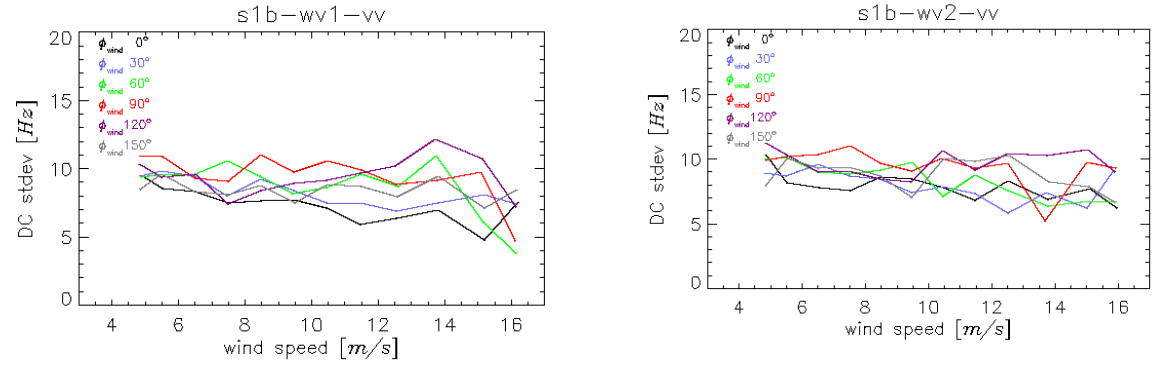

Figure 12 *S1 WV DCA RMS variations as function of wind speed and wind direction. The variations are estimated over a bin of 1m/s in wind speed and 15 degree in wind direction.*

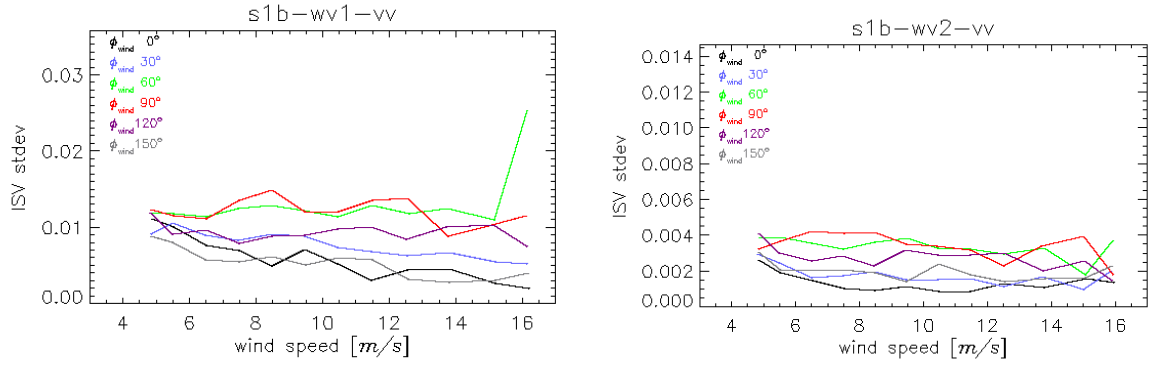

Figure 13 *S1 WV ISV RMS variations as function of wind speed and wind direction. The variations are estimated over a bin of 1m/s in wind speed and 15 degree in wind direction.*

Observation Data:

The observed data used here are the NRCS, DCA and ISV parameters for a given imaging geometry and polarization. Since we do not have real bi-static data with ground truth, we generate these using the forward models. A steady current is added to the simulated "DCA Wave Bias" using the second term of Eq.(3).

To mimic real data, we add some random noise (see Figure 11 - Figure 13) to the simulated data to mimic measurement precision (or uncertainty). This should also be dependent on the spatial resolution (or ENL) of the measurements.

Any systematic error (or bias, or accuracy) to the measurements coming from the radar system (SNR, TAR,..) are not accounted for here.

3.1.2. Cost-Function Minimization

The cost-functions are built as follows:

- Select ground truth for wind vector and current vector
- Select the observation geometry and polarization
- Extract the "observed" NRCS, DCA and ISV triplets of the S1+CS system from the look-up table of model data (netCDF).
- Add the surface current contribution to the "observed" DCA using the ground truth current vector.
- Add some random noise to the "observed" NRCS, DCA and ISV triplets.
- Access the look-up table for the model data (netCDF) and read up in memory NRCS, DCA and ISV triplets as function of wind vector corresponding to the given imaging geometry and polarization
- Access the triplets of variances of NRCS, DCA and ISV as function of wind field, corresponding to the given imaging geometry and polarization.
- Generate the total cost-function by summarizing all the individual cost-functions
- Perform a minimization of the total cost-function with respect to wind speed and direction, by interpolation on the grid of the cost-function.

3.1.3. Total surface current vector

The line-of-sight surface current components are then computed directly from the difference between the "observed" DCA and the predicted "Wave Bias DCA".

The three different line-of-sight surface current components are then combined to provide an estimate of the 2D surface current vector. An estimate of the 2D surface wind vector is also output of the cost-function minimization.

3.1.4. Flowchart

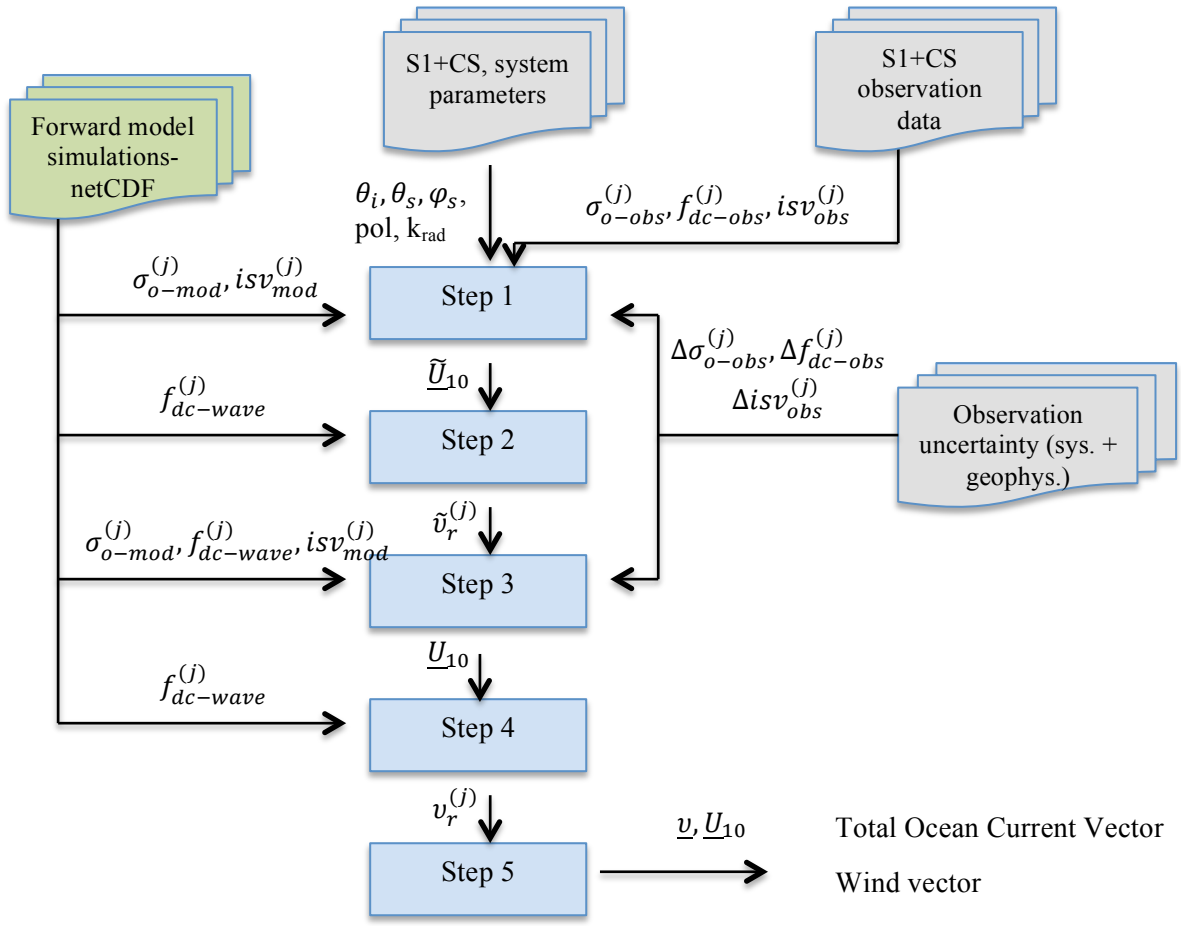

Figure 14 *Flowchart of the surface wind and current vector retrieval scheme for S1+CS constellation. Here* $j\epsilon\{cs1, s1, cs2\}$.

3.2. Test Results

The implementation has been tested by performing Monte Carlo realizations (with normal distribution of noise) for different wind speed and surface current conditions. The performance of the wind retrieval is essential for the surface current retrieval. Below we show some results of wind and current retrieval using triplets of NRCS in combination with single ISV (mono-static) value. We note that for azimuth winds the performance on the retrieved wind direction is poor. This is due to the nature of the NRCS forward model around azimuth winds and the corresponding shape of the cost-function around azimuth winds (see Figure 9).

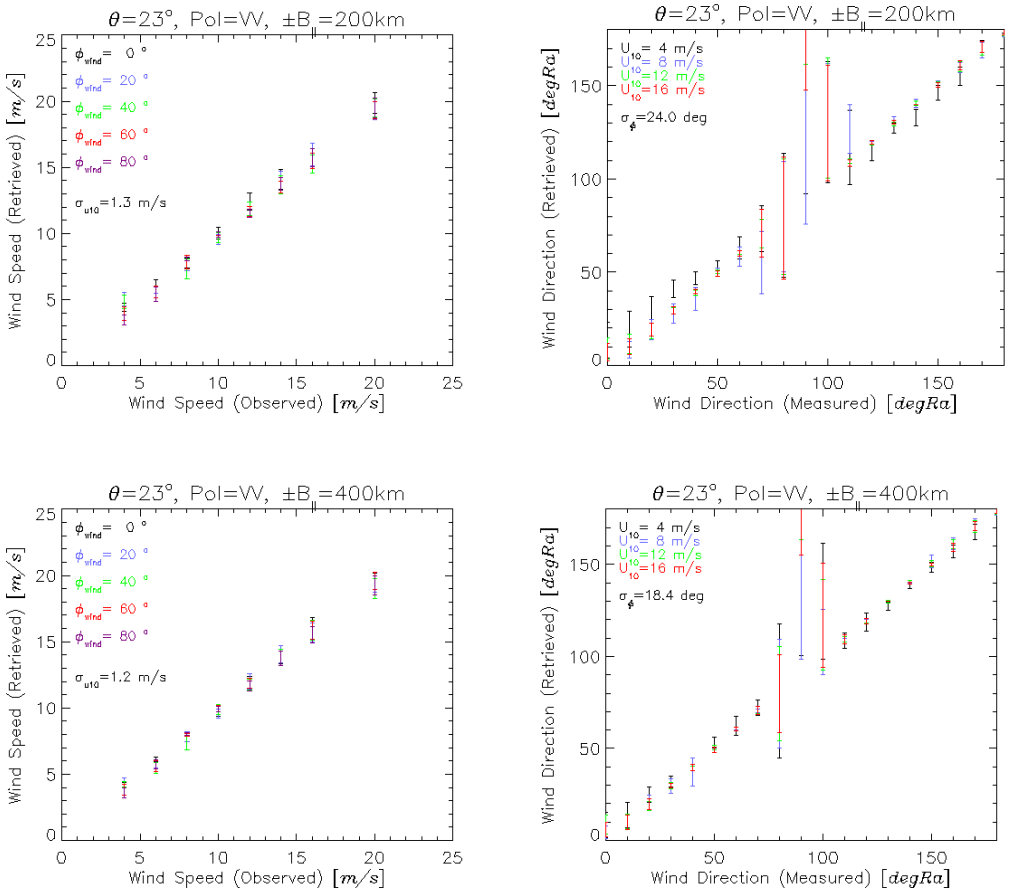

Figure 15 *Scatterplot of retrieved wind speed and direction versus input wind speed and direction. Upper plots: baseline of 200km, Lower plots: baseline of 400km.*

Figure 16 shows the standard deviations of wind speed and directions versus baseline for different incidence angles on S1. We see that the overall best performances are achieved at large baseline. In Figure 17 we show the standard deviations of current speed and directions versus baseline for different incidence angles on S1. We note that best performance is achieved at high incidence angles and large baselines.

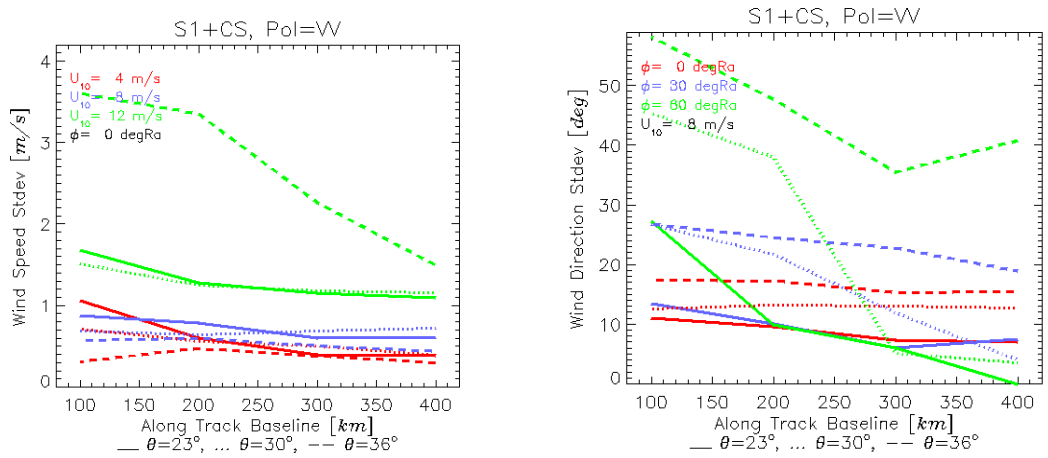

Figure 16 *Retrieved wind speed and wind direction standard deviations versus along track baseline. In left plot we set the wind direction to down wind, and in the right plot we set the wind speed to 8 m/s.*

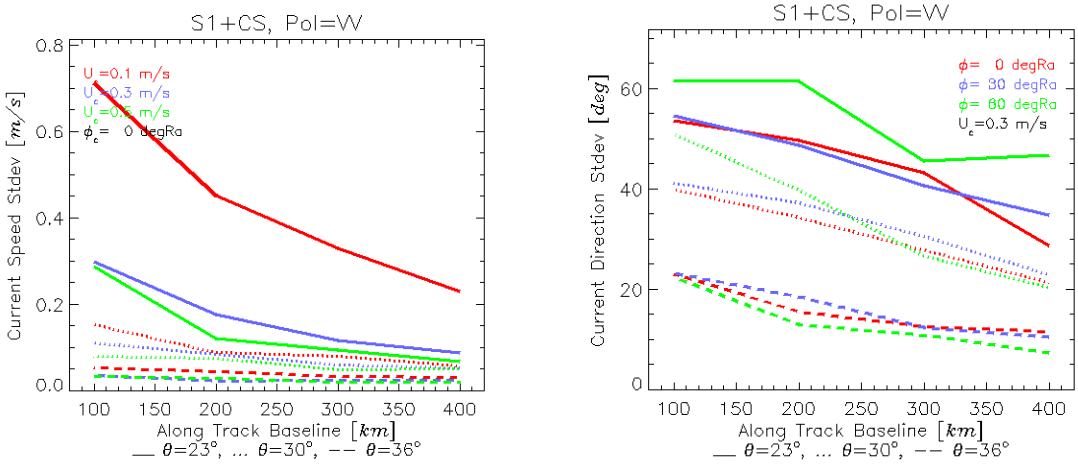

Figure 17 *Retrieved current speed and current direction standard deviations versus along track baseline. In left plot we set the current direction to positive range of master, and in the right plot we set the current speed to 0.3 m/s.*

4. Summary

A scheme for retrieval of ocean surface wind and current vectors from bistatic SAR missions are described and tested on a concept (LBS) as proposed for the HARMONY mission. The results show that use of triplets of NRCS, DCA and image cross-spectra can provide ambiguity free estimates of wind and current vectors. However, the performance of the surface current retrieval is very critical dependent on the precision of the DCA, and on the accuracy of the wind vector retrieval. In order to meet the requirements on surface current, the precision of DCA must be better than 2Hz.

We also note that best performance on OSC is achieved for high incidence angles and large baselines. This is understandable since the wind driven "DC Wave Bias" is largest at low incidence angles, and thus also the error introduced by errors in the wind vector estimate. We also see that for low current speed (0.1 m/s) the RMSe is very large, since the uncertainty of the DCA becomes of the order of the signal itself.